Demagnetization Monitoring and Identification in PM Generators With Concentrated Windings During Transient Conditions

Demagnetization Monitoring and Identification in PM Generators with Concentrated Windings During Transient Conditions

K. N. Gyftakis, T. A. Garcia-Calva, G. A. Skarmoutsos, D. Morinigo-Sotelo, M. Mueller and R. de J. Romero-Troncoso

***Abstract* – Direct drive permanent magnet machines used in renewables typically have high numbers of poles leading to low speeds. This poses a challenge for detection of faults during transients, while few periods of the operating waveforms can be captured. Moreover, it has been recently shown that the numbers of poles and stator coils determine the demagnetization harmonic generation mechanism and consequently the location of the fault signatures. This leads to different signatures in every permanent magnet machine. Additionally, the traditional signatures may not be clear in the spectrograms due to the low rotor speed. Under such conditions, the monitoring of specific higher harmonics can lead to reliable detection and identification of the demagnetization fault. The authors prove that the fault can be reliably distinguished from other rotor-related faulty conditions with the use of specific higher signatures in the stator current. Finally, the computed harmonics are experimentally verified in the lab, while the detection of demagnetization under transient conditions is achieved in this paper, that studies a double rotor axial flux PM generator as a case subject.**

***Index Terms*—Condition monitoring, Demagnetization, Fault diagnosis, Permanent magnet generators, Renewables**

I. INTRODUCTION

REMOTE renewable energy harvesting such as off-shore wind, tidal and wave gave space to direct-drive Permanent Magnet (PM) generators, in order to minimize the maintenance needs of gearboxes typically applied with induction generators [1]. These generators are typically built with a high number of poles leading to very low shaft speeds [2].

Different types of faults may appear in PM machines such as stator inter-turn faults [3], demagnetizations of the PMs [4] and a plethora of different types of mechanical faults such as eccentricities and misalignments [5], [6]. Among the rotor faults, the demagnetization one can be severe since it leads to the reduction of the air-gap magnetic flux density. Operation under fixed load conditions though will lead to operation under higher current, leading to additional thermal stress and further demagnetization severity until the machine collapses [7]. It is therefore crucial to detect the fault at an incipient level and plan fault tolerance and maintenance actions appropriately.

Partial demagnetization usually originates from defective manufacturing of the PMs or some damage during the assembly of the generator [8], [9]. High loading or thermal stress will build on those defects and lead to the permanent demagnetization of the PMs [10].

In the literature, one can find works dealing with the detection of demagnetization faults. Mostly applied methods are the Motor Current Signature Analysis (MCSA) [11], [12] and the magnetic flux analysis, either air-gap or stray [13], [14]. However, most papers deal with high speed PM machines where the number of poles is small and the fault related signatures are specific and few. More importantly, the demagnetization fault signatures coincide with the rotor mechanical fault ones leading to identification issues [15], [16]. Moreover, past papers focus on the analysis of the PM machines at steady state.

Frequency signature analysis is severely influenced by the winding configuration [20], and the slot number as these harmonics are influenced by the harmonics, which are generated by the slotting effect [21]. Under healthy conditions, the spatial distribution of the coil/pole slot combination significantly affects the harmonic content of voltage through the winding factor [22], in machines with and without armature core. Specifically, in machines with parallel path windings under fault conditions the magnetic field along the air-gap circumference ceases to be symmetric, as a result circulating currents on the branches of a phase generate, distorting the current waveform [23] and influencing the unbalanced magnetic pull [24]. Therefore, the amplitudes of the fault signatures are much dependent on the design parameters of the machine, rending the diagnostic process unreliable.

K. N. Gyftakis is with the School of Electrical and Computer Engineering, Technical University of Crete, 73100, Greece (e-mail: k.n.gyftakis@ieee.org)

G. A. Skarmoutsos and M. Mueller are with the School of Engineering and the Institute for Energy Systems, University of Edinburgh, Edinburgh, EH9 3FB, UK (e-mail: g.a.skarmoutsos@ieee.org, Markus.Mueller@ed.ac.uk).

T. A. Garcia-Calva is with the Electronic Engineering Department, University of Guanajuato, GTO 36700 MX (e-mail: ta.garciacalva@ugto.mx).

D. Morinigo-Sotelo is with the Electrical Engineering Department, University of Valladolid, Valladolid VLL 47002 ES (e-mail: daniel.morinigo@eii.uva.es).

R. de J. Romero-Troncoso is with the Mechatronics Engineering Department, Autonomous University of Querétaro, San Juan del Río, QRO 76806 MX (e-mail: troncoso@hspdigital.org).

However, PM machines utilized in renewables, experience continuous transients making the steady state techniques unreliable or not easily applied. Moreover, the well-known frequencies adopted in the literature are sub-harmonics of the fundaments creating resolution issues since the low speed does not permit the capturing of enough periods for significant spectral resolution. Fault analysis under transient operating conditions can be detected using time-frequency based signal processing algorithms in which every algorithm uses different transformation functions.

Furthermore, in such cases the captured signals cease to be periodic, so other signal processing algorithms have been proposed for condition monitoring. STFT [25] has a steady window length, so fast transients cannot be analyzed with high resolution and can be combined using Neuro-Fuzzy approach [26]. Therefore, for signals with rapid alterations, Continuous and Discrete Wavelet Transforms (CWT, DWT) are more appropriate as the window length is variable [27][28]. Other time-frequency distributions methods based on the quadratic time-frequency distribution [29], Hilbert-Huang transform, which are capable of analyzing the signal from a time-frequency-energy aspect. Moreover, the demagnetization fault can also be identified using features extracted by CWT and analyzed by the box-counting method and a threshold [30]. Finally, a recent paper [31] utilizes the recursive least-squares (RLS) method to detect the demagnetization fault in a high speed motor and offers some identification with respect to the dynamic eccentricity fault.

Aiming to answer those needs, this paper which is the continuation of the early work [32], investigates the use of the stator current for condition monitoring during transient operation of PM generators. Firstly, analytical calculations will demonstrate the expected higher harmonics as a function of the machines' stator coils and numbers of poles. Then, the case of an axial flux PM generator will be examined with the use of Finite Element Analysis (FEA) and the stator current waveforms will be extracted and analysed with a high-resolution spectral decomposition. The machine will be subjected to a variety of faults such as partial demagnetization, axial and radial misalignments and eccentricities. The results will show that the monitoring of specific higher harmonics in the stator current can be an excellent method to detect and identify the partial demagnetization fault.

II. Analytical Investigation

In order to calculate the signatures induced to the stator due to the demagnetization fault, the air-gap magnetic flux density is needed and it is given by equation (1).

$$B_{AG} = \Lambda \cdot F_m \tag{1}$$

where:

$$F_m(\theta,t) = \sum_{n=2m+1}^{\infty} F_{PM} \cos(np\theta - n\omega_s t - \varphi_n) \tag{2}$$

and the permeance due to one magnet demagnetized [17]:

$$\Lambda_{dmg}(\theta,t) = \alpha + \beta(D) + \gamma(D)\sum_{k=1}^{\infty}\cos(k\theta - k\omega_r t) \tag{3}$$

where:

$$\alpha = \frac{\mu_0}{2h_{PM}}\left(1 - \frac{g}{h_{PM}} - \frac{t_w}{2h_{PM}} + \frac{g^2}{h_{PM}^2} + \frac{gt_w}{h_{PM}^2} + \frac{t_w^2}{4h_{PM}^2}\right)$$

$$\beta(D) = \frac{\mu_o D}{2h_{PM}}\left(\frac{g}{2h_{PM}^2 p} + \frac{t_w}{4h_{PM} p} - \frac{1}{2h_{PM} p}\right)$$

$$\gamma(D) = \frac{\mu_o}{2h_{PM}}\left\{\left(\frac{D}{2h_{PM} p} + \frac{2g}{h_{PM}} + \frac{t_w}{h_{PM}} - 1\right)\sum_{k=1}^{\infty}\frac{D}{k\pi h_{PM}}\sin\left(\frac{k\pi}{2p}\right)\right\}$$

Therefore, the air-gap magnetic flux density due to (1), (2) and (3) is given by:

$$B(\theta,t) = \sum_{n=2m+1}^{\infty} F_{PM}\cos(np\theta - n\omega_s t - \varphi_n) + \beta_k \sum_{n=2m+1}^{\infty}\sum_{k=1}^{\infty}\left\{F_{PM}\alpha_k\left[\begin{array}{l}\cos\left((np-k)\theta - \left(n+\frac{k}{p}\right)\omega_s t - \varphi_n\right) + \\ \cos\left((np+k)\theta - \left(n+\frac{k}{p}\right)\omega_s t - \varphi_n\right)\end{array}\right]\right\} \tag{4}$$

where:

$$\alpha_k = a + \beta(D)$$

$$\beta_k = \frac{\gamma(D)}{2}$$

Furthermore, the magnetic flux can be calculated by:

$$\Phi = \iint \mathrm{B}\, dS \tag{5}$$

This flux will induce an Electromotive Force (EMF) to each stator winding, which is described by (6)

$$V_{dmg} = \sum_{n=2m+1}^{\infty} V_n \cos(np\theta - n\omega_s t - \varphi_n) + \sum_{n=2m+1}^{\infty}\sum_{k=1}^{\infty}\left\{V_{nk}\left[\begin{array}{l}\cos\left((np-k)\theta - \left(n-\frac{k}{p}\right)\omega_s t - \varphi_n\right) + \\ \cos\left((np+k)\theta - \left(n+\frac{k}{p}\right)\omega_s t - \varphi_n\right)\end{array}\right]\right\} \tag{6}$$

Depending on the stator windings number and their spatial location with respect to each other, the following signatures

are generated [18]:

- $f_{dmg1} = \left(n \pm \frac{2^{\delta} \varepsilon}{p} \right) f_s$, if the phase coils are a power of 2 (defined by δ).
- $f_{dmg2} = \left(n \pm \frac{3k}{p} \right) f_s$, if the phase coils number is a multiple of 3.

Moreover, the harmonics obeying to: $f_{3ph\_null} = \frac{3\gamma\lambda'}{p} f_s$, (γ is the number of phase coils) are expected to disappear due to the three phase winding.

III. Finite Element Analysis at Steady State

For the purposes of this work, an axial flux PM generator has been simulated with FEA under steady state and transient operating conditions. The generator has a distributed winging with 3 coils per phase while p=6. So, it becomes clear that due to its manufacturing characteristics, this machine will generate demagnetization signatures according to f_{dmg2}.

The PM machine and the FEA model are shown in Fig. 1. It has been analyzed under healthy and faulty condition. The level of partial demagnetization has been 35% and affects a single magnet.

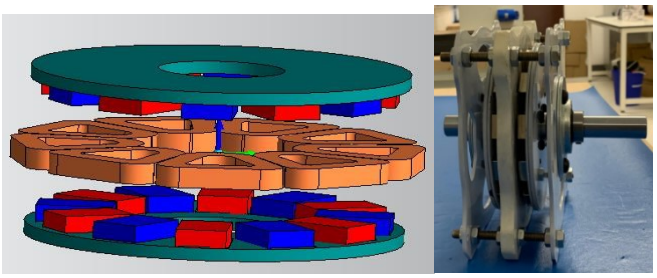

a) b)

Fig. 1. a) The FEA model and b) the real generator.

The generator is simulated to operate at steady state first, aiming to validate the formulae and identify the demagnetization harmonics in the stator current spectra, which are depicted in Fig. 2. For this machine p=6, so the expected fault-related harmonics are given for different values of the integer κ: $f_s - \frac{f_s}{2}$, $f_s + \frac{3f_s}{2}$ and $f_s + \frac{5f_s}{2}$. The signature at $f_s + \frac{f_s}{2}$ is indeed produced in each phase but cancels out due to the three phase winding as predicted by f_{3ph_null} above.

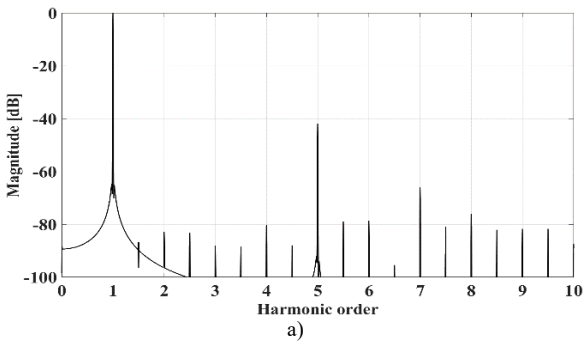

a)

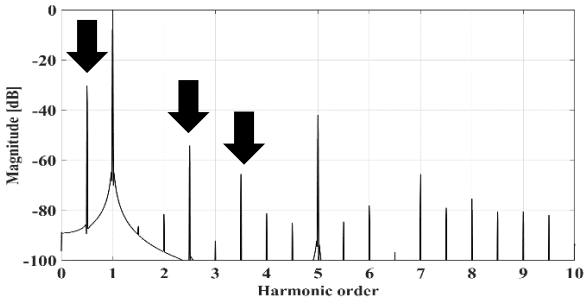

b)

Fig. 2. Stator current spectra at steady state: a) healthy and b) demagnetization conditions.

IV. Transient Analysis

A. Time-frequency Analysis

A class of high-resolution techniques based on an eigen decomposition of an autocorrelation matrix of the data signal have been promoted in recent literature as having better resolution and better frequency-estimation characteristics than classical frequency estimators such as Fourier transform [19]. The Min-Norm algorithm is a high-resolution technique based on harmonic decomposition of multi-component signals. A multi-component signal z can be expressed as:

$$z(l) = \sum_{m=1}^{\infty} v(\psi_m) s_m(l) + \eta(l) \tag{7}$$

where $s_m(l)$ denotes the m-th component in the signal, $m \in R$, $v(\psi_m)$ the discrete frequencies vector, [$\varphi \in R$), and $\eta(l)$ the noise in the measured signal. The power spectral density (PSD) of z is given by [20]:

$$PSD_{MN}(\psi) = \frac{1}{\left| v^H(\psi) \psi^2 \right|} \tag{8}$$

where $\boldsymbol{\psi}$ belongs to the sample noise subspace, has minimum norm, and the first element equal to 1. The Min-Norm algorithm reduces anomalies (spurious peaks) in spectral estimates exhibit in other high-resolution techniques such as Pisarenko harmonic decomposition or the Multiple signal classification algorithms. The time-frequency distribution of the stator current is computed by sectioning the data sequence into smaller segments, taking the autocorrelation of each subsequence, and evaluating the PSD.

The proposed method was implemented under MATLAB in a PC with Intel Core i5 at 1.6 GHz. The methodology is composed of four stages: analog to digital conversion, sample rate conversion, signal windowing, and spectral analysis. Once the current signal is acquired for 1 second, the complete method requires 146 msec to compute its time-frequency decomposition. The block diagram of the methods application is shown in Fig. 3 below.

This article has been accepted for publication in IEEE Transactions on Industry Applications. This is the author's version which has not been fully edited and content may change prior to final publication. Citation information: DOI 10.1109/TIA.2022.3221699

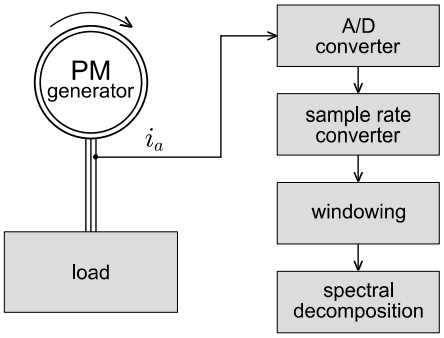

Fig. 3. Simplified block diagram of the method.

B. *FEA Analysis and Examined Cases of Rotor Faults*

In this section the test-machine is modelled using 3-D FEA software, named Simcenter MagNet by Siemens digital industries. Axial-flux machines, unlike radial-flux machines, can only be modelled reliably using 3-D modeler, since the scalar and vector magnetic potentials alter along all directions. Another advantage of the 3-D simulations is that the stator-end winding fields are accounted in the field solution. Hence, this method of modelling is considered the most accurate, with the disadvantages that is time-consuming and occasionally divergent due to the high complexity of the volume mesh grid. By solving the model using the transient with motion analysis the phase quantities in the time domain are obtained. A Fast-Fourier Transform (FFT) algorithm is then used to calculate the frequency spectra for the stationary signals.

The faults are implemented as follows. The partial demagnetization fault is inserted in the machine by reducing the slope of the PM's magnetic characteristic. The magnetic characteristic of rare-earth magnets is approximately linear on the second quadrant at 20° [C]. By reducing the slope of the line, common point of the load line and characteristic reduces, consequently a demagnetization fault which is equal with the percentage of the slope reduction can be implemented. The axis misalignment faults are implement by displacing the rotor disc parallel to the stator disc. For static axis misalignment, the rotor axis of rotation should be the same with the axis of the displacement. For dynamic axis misalignment, the rotor axis of rotation should be the same with the stator's axis after the displacement. In this fault, a portion of the magnetic flux tends to leaves the surface of the stator coils. With the same concept the angular misalignment faults can be implemented with the only difference that a rotor disc is twisted relatively to the stator disc. In this case the air-gap becomes non-uniform. Fig. 4 illustrates the angular and axis misalignment for each eccentricity case. Table I illustrates the major specifications for the studied axial-flux generator.

TABLE I
MAJOR SPECIFICATIONS OF THE AFPM GENERATOR

Parameter	VALUE
Apparent Power [VA]	45
Torque [Nm]	0.5
Rotational speed [r/min]	500
Pole pairs/ Coils	6/9
Turn number of armature	16
Winding connection	Y
Magnet-coil clearance [mm]	2
Magnet remanence (20 °C) [T]	1.35
Inner/Outer magnet radius [mm]	40/70

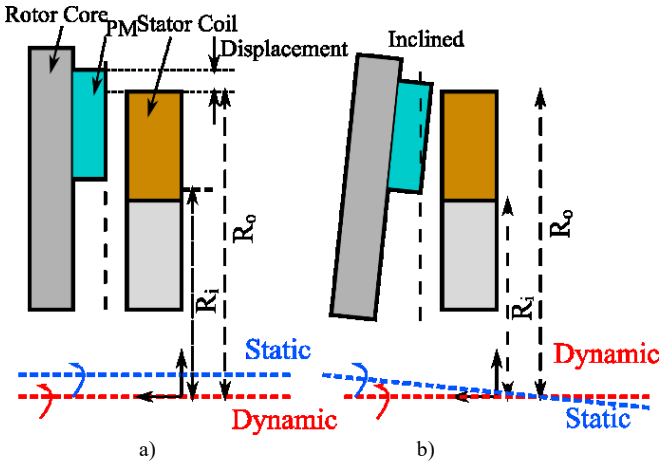

Fig. 4. Graphical representation of the: a) axis and b) angular misalignment giving emphasis to the axis of rotation for static and dynamic eccentricity.

C. *Analysis Results of Rotor Faults*

The simulation scheme allows a detailed analysis of the machine behavior under several fault conditions. A Time-frequency (*t-f*) analysis based on the Min-Norm technique is applied to the stator current signals for tracking the presence of fault-related harmonics. The analyzed stator current signals correspond to 0.4 seconds of transient operation and a logarithmic scale in dB is used to visualize the full range of the spectral content.

Under healthy condition where there is no abnormality in the PM generator, the largest magnitude component of the analyzed current is the fundamental mode f_s, whose instantaneous frequency changes as time evolves with positive slope of 75 Hz/sec as can be seen in Fig. 5. The spectrogram also exhibits the presence of a spectral line evolution from 100 to 250 Hz corresponding to the 5th harmonic of f_s. This result coincides with the steady state analysis in Fig. 2.a.

This article has been accepted for publication in IEEE Transactions on Industry Applications. This is the author's version which has not been fully edited and content may change prior to final publication. Citation information: DOI 10.1109/TIA.2022.3221699

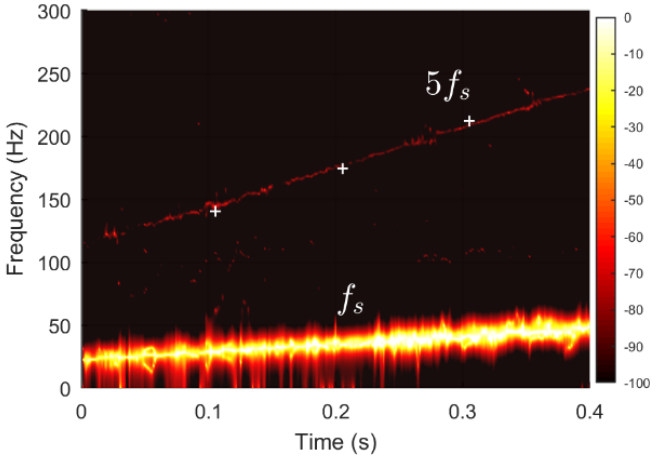

Fig. 5. *T-f* decomposition of the stator current at transient state: healthy condition.

The behavior of the PM generator under partial demagnetization of a single magnet is presented in Fig. 6., the *t-f* decomposition shows the appearance of a high-power signature below the fundamental component f_s, which seem to be the f_s-$f_s/2$ fault-related harmonic, but the spectral signature is not accurately localized in the *t-f* plane because it is very close to the f_s. However, above f_s a demagnetization harmonic located at $f_s+3f_s/2$ can be easily identified. Although this fault-related harmonic has lower energy concentration than the $0.5f_s$ mode, it does not suffer from interference problem of the fundamental component. As expected, $f_s+f_s/2$ is not present in the signal due to the winding configuration. Also note that the *t-f* decomposition generates a weaker harmonic component between the $5f_s$ and $2.5f_s$ trajectories that appears to be the 3.5 f_s fault-related and is the result of $f_s+5f_s/2$.

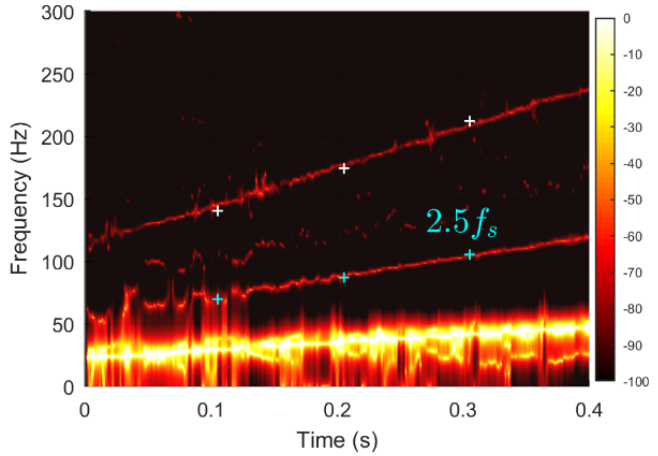

Fig. 6. *T-f* decomposition of the stator current at transient state: 20% Partial Demagnetization.

Fig. 7. and Fig. 8. depict the stator current's *t-f* decompositions under two simulated dynamic misalignment fault conditions. Fig. 7 depicts a plot of the *t-f* decomposition for 2 mm of dynamic axis misalignment, whereas Fig. 8. shows the *t-f* distribution for 40% of dynamic angular misalignment. In both cases, the spectral contents of the currents are very similar except that the axis misalignment case (Fig. 7) presents spectral shapes crossing the 5th harmonic, but they are almost indistinguishable in the time-frequency distribution.

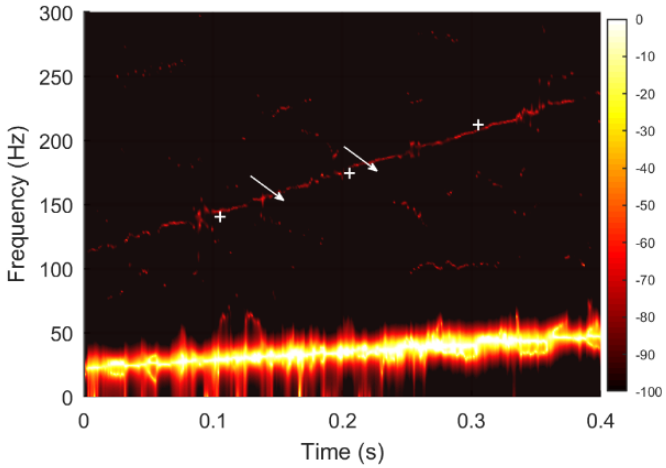

Fig. 7. *T-f* decomposition of the stator current at transient state: 2mm dynamic axis misalignment.

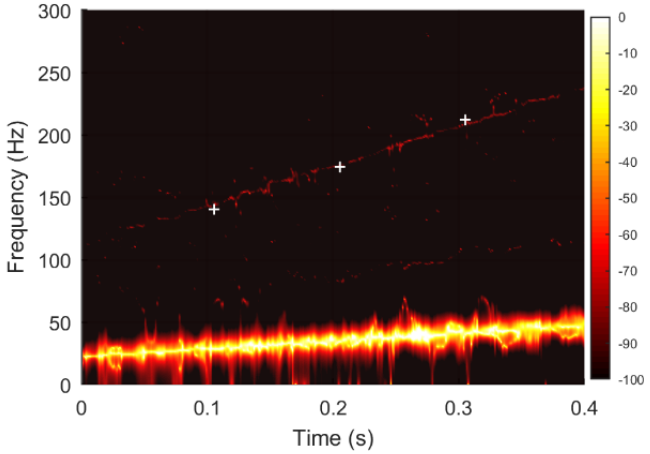

Fig. 8. *T-f* decomposition of the stator current at transient state: 40% dynamic angular misalignment.

Finally, the transient analysis technique was implemented to the simulated PM generator under two static misalignment faults. The results of the analysis of axial and angular misalignments are presented in Fig. 9 and Fig. 10, respectively. The fundamental component and the 5th harmonic are present and with large amplitudes in both time-frequency decompositions. If the spectrogram of the axial misalignment condition (Fig. 9) is compared with the healthy case (Fig. 5), it is observed an increase in spectral energy above the 5th component.

This article has been accepted for publication in IEEE Transactions on Industry Applications. This is the author's version which has not been fully edited and content may change prior to final publication. Citation information: DOI 10.1109/TIA.2022.3221699

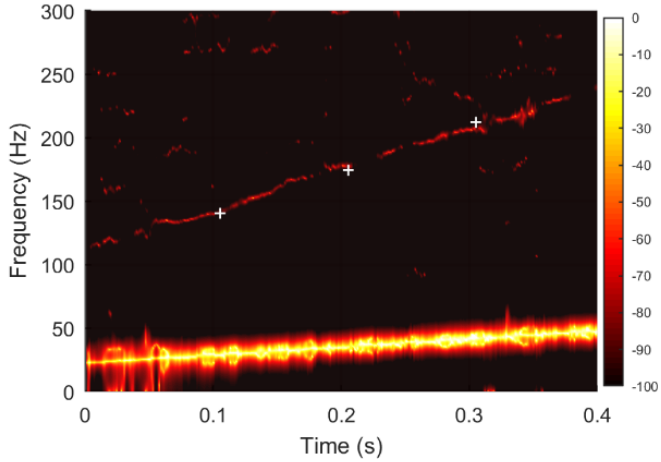

Fig. 9. *T-f* decomposition of the stator current at transient state: 1 mm static axis misalignment.

On the other hand, in the case of angular misalignment condition, the PM generator generates different signatures in the stator current spectrogram, components with abrupt changes in frequency are observed in the spectral band between 50 and 300 Hz (see Fig. 10), indicating the presence of very small spikes in the stator current signal.

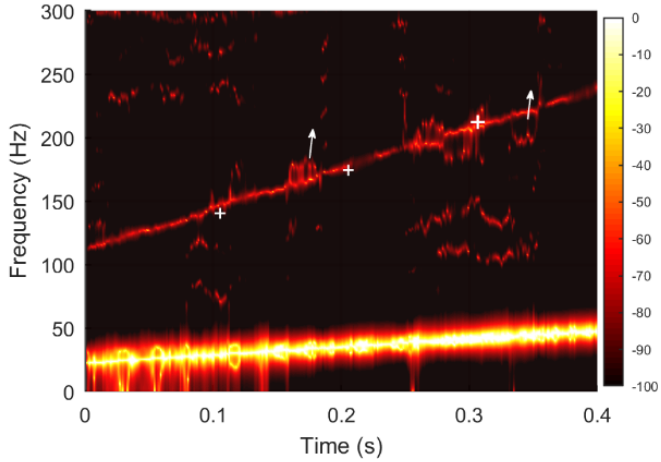

Fig. 10. *T-f* decomposition of the stator current at transient state: 20% static angular misalignment.

Among the spectrograms, results of several fault conditions, the transient analysis of the PM generator under partial demagnetization, has been shown to exhibit a particular signature pattern in the time-frequency domain. The transient analysis of the stator current permitted distinguish unequivocally the demagnetization condition not only from the healthy state, but also from other fault conditions.

D. Stator Inter-Turn Faults and Analysis

The generator model has been modified to represent stator inter-turn faults of two different severities (2 and 3 shorted turns) in phase A. The contact resistance is 0.1 Ω. The stator current has been extracted from both models and their spectrograms are shown in Fig. 11 below. It is clear that, the 5th harmonic increases in amplitude, however there is absolutely no presence of any of the demagnetization signatures (no signature at $0.5f_s$, $2.5f_s$, or $3.5f_s$).

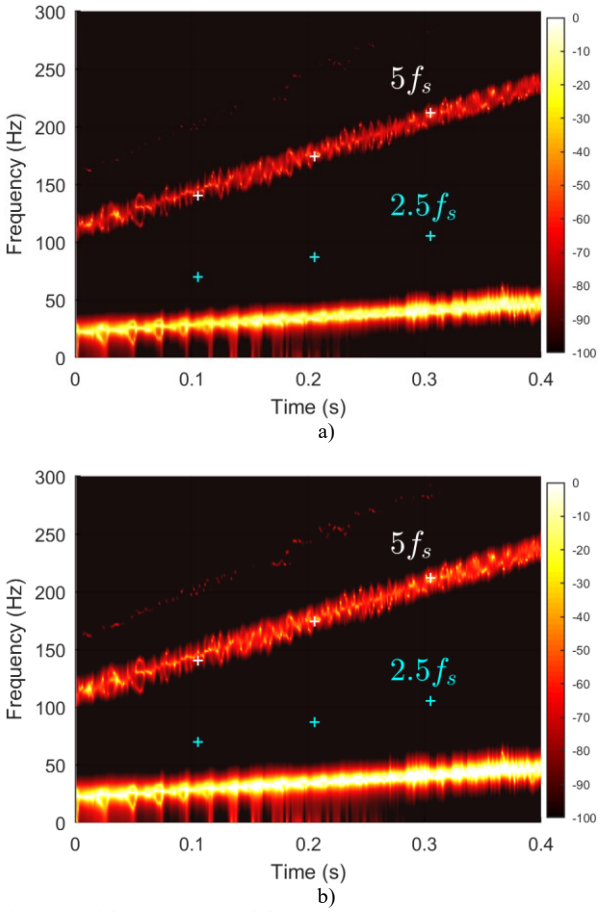

Fig. 11. *T-f* decomposition of the stator current at transient state: a) 2 turns shorted and b) 3 turns shorted in one phase of the stator.

V. Experimental Testing

To validate the proposed signal processing technique a test bed was created to capture the signal of the stator current under various faulty conditions on a transient state. The proposed test bed is illustrated in Fig. 12. It consists of a 3-phase voltage inverter, which drives a 3-phase induction motor. The induction motor is the prime mover to the tested axial-flux permanent-magnet generator, which supplies a variable, 3-phase resistive load. To acquire the signals of the stator current, a data-acquisition-system employing current probes has been adopted.

This article has been accepted for publication in IEEE Transactions on Industry Applications. This is the author's version which has not been fully edited and content may change prior to final publication. Citation information: DOI 10.1109/TIA.2022.3221699

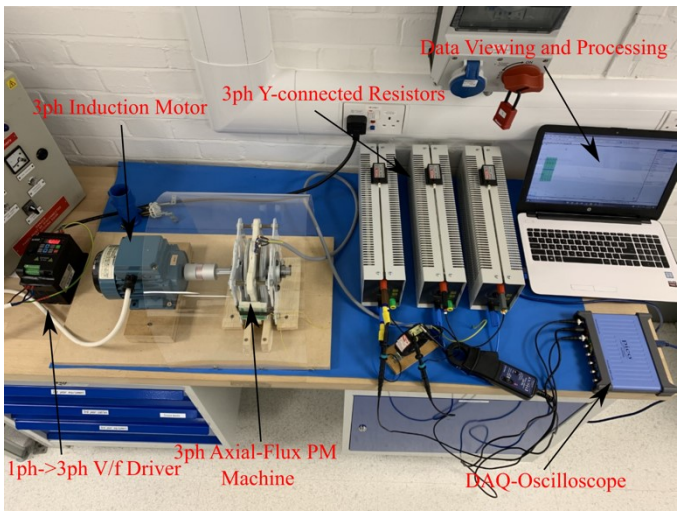

Fig. 12. Experimental layout of the test axial-flux PM machine.

To verify the feasibility of the analysis, three different conditions are tested: healthy state, one magnet demagnetized and one with dynamic angular misalignment. The demagnetization fault was created by removing a magnet from one of the rotor discs. Since it is a double sided disc generator, every pole pitch is occupied by two magnets, hence a 50% partial demagnetization has been created. The dynamic angular misalignment is implemented by adding washers on two out of four bolts, which tie a rotor disc with the axis of the machine. In order for the rotor discs, to be angularly rotatable, the opposite inner diameter of a disc was filled to create enough clearance.The experimental tests realize an ascending speed curve starting from standstill for all the studied conditions. Spectrograms of the stator currents are presented in the same frequency bandwidth for comparison purposes, the short-time analysis have been performed by the Min-Norm algorithm with a window length of 128 samples, a leap of 2 samples between successive windows, and a low-frequency band analysis. In addition, it should be specified that the original sampling frequency (f_n =25kHz) is converted to f_n=f_n/20 in this study to reduce the computational burden.

In Fig. 13, the *t-f* decomposition of the stator current signal for the healthy case is shown. It can be seen from the result that the stator current consists of the fundamental component f_s, which is embedded in a high level of noise. It is known that the instantaneous frequency of f_s is directly proportional to the instantaneous speed of the PM generator, which can reflect the motion behavior of the machine. In this case, there are linear speed changes appearing as linear FM segments in the *t-f* distribution of the stator current.

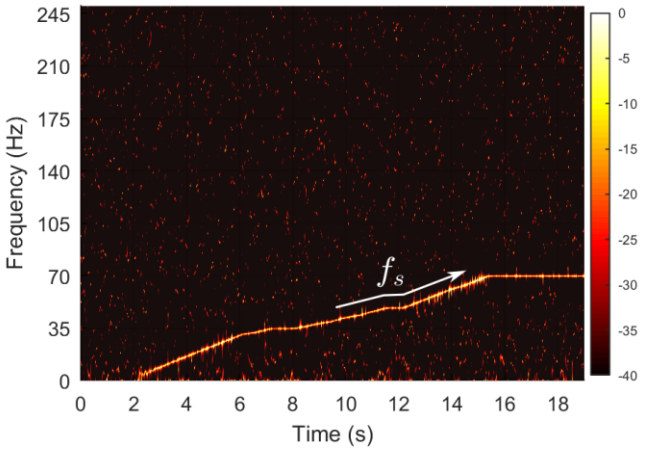

Fig. 13. *T-f* decomposition of the stator current at non-stationary conditions: healthy condition.

The time-frequency decomposition of the stator current under faulty condition is shown in Fig. 14. The fundamental component reflects a time-varying behavior of the PM machine, similar to the experimental result in Fig. 13. However, the decomposition reveals supplementary information. The energy around f_s and the DC component seems to have an increment. But more important is the fact that the three fault signatures predicted earlier, 0.5 *fs*, 2.5*fs* and 3.5 *fs* emerge from the noise floor of the *t-f* decomposition and displays the trajectories corresponding to the demagnetization fault at f_{dmg2} (for k =1, 3, and 5). It worth to mentioning that at low speeds spectral density around f_s and DC could overlap with the fault signature 0.5 f_s, leading to a false diagnostic. On the other hand, high harmonics present a larger spectral distance between other components.

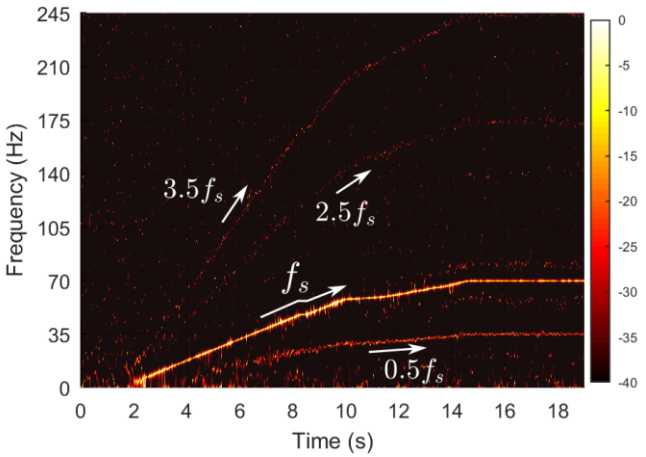

Fig. 14. *T-f* decomposition of the stator current at non-stationary conditions: demagnetized condition.

Finally, Fig. 15 illustrates the time-varying spectrum for the rotor misaligned case. The FM law for f_s is clear from the sharp resolution of the decomposition. However, the stator current does not contain any other oscillatory component. Experimental results show that indeed the time-frequency analysis allows detection and discrimination between the demagnetization condition and other PM generator conditions.

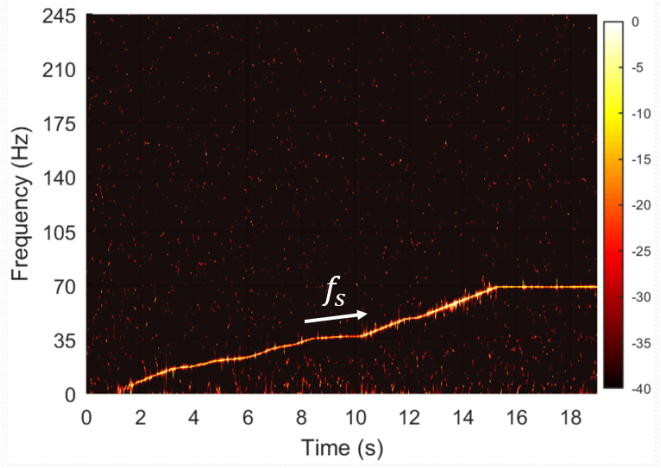

Fig. 15. T-f decomposition of the stator current at non-stationary conditions: dynamic angular misalignment condition.

Although subspace methods improve the frequency estimation performance, computational complexity is one important factor for practical applications. In this study, high-resolution results were obtained applying the short-time minimum algorithm to stator current signals. The time-frequency plots shown in Fig. 13, Fig. 14 and Fig. 15 have been computed in 11.48, 11.69, and 11.87 seconds, respectively. Considering that the analyzed signal lengths are 19 seconds, it can be concluded that, the computational time is not a problem for analyzing non-stationary signals. Time-frequency decompositions were computed in a PC with an Intel Core i7 processor.

VI. Conclusions

This paper demonstrates the advantageous use of higher stator current harmonics for the detection of partial demagnetizations faults in low speed direct drive PM generators. While those generators are utilized in renewable energy harvesting, they experience continuous transients therefore conventional steady state diagnostic approaches cannot be applied. It is shown in the paper that the Min-Norm decomposition is capable not only of detecting the partial demagnetization fault but reliably distinguishing it from other common rotor-related faulty conditions such as static and dynamic misalignment and eccentric conditions. A synopsis of the new elements to the diagnostics community, offered by this research paper are summarized below:

- Fault detection of demagnetization during the transient operation of the PM machines using the Minimum Norm algorithm.
- Discrimination between the demagnetization fault and other rotor and stator faults during transient operation.
- Strategic selection of the appropriate signatures for fault detection depending on the monitored stator current signal parameters. At steady state, the expected signatures are clearly observed. However, when it comes to fault detection under transient conditions, the low speed does not allow enough periods of the signal to be captured in time. This may lead to poor resolution of the frequency area to the left of the fundamental where the strongest fault signatures exist. The use of the analytical investigation offers a solution because it permits the identification of other harmonics at higher frequencies that can reveal the fault reliably.

VII. References

[1] H. Polinder, J. A. Ferreira, B. B. Jensen, A. B. Abrahamsen, K. Atallah, and R. A. McMahon, "Trends in wind turbine generator systems," *IEEE J. Emerg. Sel. Top. Power Electron.*, vol. 1, no. 3, pp. 174–185, 2013.

[2] A. Di Gerlando, G. Foglia, M. F. Iacchetti, and R. Perini, "Axial flux PM machines with concentrated armature windings: Design analysis and test validation of wind energy generators," *IEEE Trans. Ind. Electron.*, vol. 58, no. 9, pp. 3795–3805, 2011.

[3] J. Faiz, H. Nejadi-Koti, and Z. Valipour, "Comprehensive review on inter-turn fault indexes in permanent magnet motors," *IET Electr. Power Appl.*, vol. 11, no. 1, pp. 142–156, 2017.

[4] J. Faiz and E. Mazaheri-Tehrani, "Demagnetization Modeling and Fault Diagnosing Techniques in Permanent Magnet Machines under Stationary and Nonstationary Conditions: An Overview," *IEEE Trans. Ind. Appl.*, vol. 53, no. 3, pp. 2772–2785, 2017.

[5] J. Faiz and H. Nejadi-Koti, "Eccentricity fault diagnosis indices for permanent magnet machines: State-of-the-art," *IET Electr. Power Appl.*, vol. 13, no. 9, pp. 1241–1254, 2019.

[6] M. Thiele and G. Heins, "Computationally Efficient Method for Identifying Manufacturing Induced Rotor and Stator Misalignment in Permanent Magnet Brushless Machines," vol. 52, no. 4, pp. 3033–3040, 2016.

[7] J. C. Urresty, R. Atashkhooei, J. R. Riba, L. Romeral, and S. Royo, "Shaft trajectory analysis in a partially demagnetized permanent-magnet synchronous motor," *IEEE Trans. Ind. Electron.*, vol. 60, no. 8, pp. 3454–3461, 2013.

[8] A. A. El-Moneim, A. Gebert, F. Schneider, O. Gutfleisch, and L. Schultz, "Grain growth effects on the corrosion behavior of nanocrystalline NdFeB magnets," *Corros. Sci.*, vol. 44, no. 5, pp. 1097–1112, 2002.

[9] J. Hong, D. Hyun, S. Bin Lee, J. Y. Yoo, and K. W. Lee, "Automated monitoring of magnet quality for permanent-magnet synchronous motors at standstill," *IEEE Trans. Ind. Appl.*, vol. 46, no. 4, pp. 1397–1405, 2010.

[10] S. Ruoho, J. Kolehmainen, J. Ikäheimo, and A. Arkkio, "Interdependence of demagnetization, loading, and temperature rise in a permanent-magnet synchronous motor," *IEEE Trans. Magn.*, vol. 46, no. 3 PART 2, pp. 949–953, 2010.

[11] J. C. Urresty, J. R. Riba, M. Delgado, and L. Romeral, "Detection of demagnetization faults in surface-mounted permanent magnet synchronous motors by means of the zero-sequence voltage component," *IEEE Trans. Energy Convers.*, vol. 27, no. 1, pp. 42–51, 2012.

[12] S. Rajagopalan, W. le Roux, T. G. Habetler, and R. G. Harley, "Dynamic eccentricity and demagnetized rotor magnet detection in trapezoidal flux (Brushless DC) motors operating under different load conditions," *IEEE Trans. Power Electron.*, vol. 22, no. 5, pp. 2061–2069, 2007.

[13] T. Goktas, M. Zafarani, K. W. Lee, B. Akin, and T. Sculley, "Comprehensive Analysis of Magnet Defect Fault Monitoring Through Leakage Flux," *IEEE Trans. Magn.*, vol. 53, no. 4, 2017.

[14] A. Mohammed, J. I. Melecio, and S. Durovic, "Electrical Machine Permanent Magnets Health Monitoring and Diagnosis Using an Air-Gap Magnetic Sensor," *IEEE Sens. J.*, vol. 20, no. 10, pp. 5251–5259, 2020.

[15] R. Z. Haddad and E. G. Strangas, "On the Accuracy of Fault Detection and Separation in Permanent Magnet Synchronous Machines Using MCSA/MVSA and LDA," *IEEE Trans. Energy Convers.*, vol. 31, no. 3, pp. 924–934, 2016.

[16] W. Le Roux, R. G. Harley, and T. G. Habetler, "Detecting Rotor Faults in Low Power Permanent Magnet Synchronous Machines," *IEEE Trans. Power Electron.,* vol. 22, no. 1, 2007.

[17] G. Skarmoutsos, K. N. Gyftakis, and M. Mueller, "Detecting partial demagnetization in AFPM generators by monitoring speed and EMF induced in a supplemental winding," *IEEE Trans. Ind. Inform.,* Vol. 18, No. 5, pp. 3295-3305., 2022.

[18] K. N. Gyftakis, S. Rasid, G. A. Skarmoutsos and M. Mueller, "The Demagnetization Harmonics Generation Mechanism in Permanent Magnet Machines with Concentrated Windings", *IEEE Trans. Ener. Conv.,* Vol. 36, No. 4, pp. 2934-2944., 2021.

[19] S. Lawrence Marple Jr., "Digital Spectral Annalysis," 2nd ed., Ed. New York: Dover Publications, Inc., 2019, pp. 15-64.

[20] T. A. Garcia-Calva, D. Morinigo-Sotelo, O. Duque-Perez, A. Garcia-Perez, and R. de J. Romero-Troncoso, " Time-Frequency Analysis Based on Minimum Norm Spectral Estimation to Detect Induction Motor Faults," Energies, vol. 13, Aug. 2020.

[20] T. Goktas, M. Zafarani, K. W. Lee, B. Akin, and T. Sculley, "Comprehensive Analysis of Magnet Defect Fault Monitoring Through Leakage Flux," IEEE Trans. Magn., vol. 53, no. 4, 2017.

[21] J. C. Urresty, J. R. Riba, and L. Romeral, "Influence of the stator windings configuration in the currents and zero-sequence voltage harmonics in permanent magnet synchronous motors with demagnetization faults," IEEE Trans. Magn., vol. 49, no. 8, pp. 4885–4893, 2013.

[22] M. J. Kamper, A. J. Rix, D. A. Wills, and R. J. Wang, "Formulation, finite-element modeling and winding factors of non-overlap winding permanent magnet machines," Proc. 2008 Int. Conf. Electr. Mach. ICEM'08, no. 3, pp. 1–5, 2008.

[23] E. Maruyama, A. Nakahara, A. Takahashi, and K. Miyata, "Circulating current in parallel connected stator windings due to rotor eccentricity in permanent magnet motors," 2013 IEEE Energy Convers. Congr. Expo. ECCE 2013, pp. 2850–2855, 2013.

[24] I. P. Brown, D. M. Ionel, and D. G. Dorrell, "Influence of parallel paths on current-regulated sine-wave interior-permanent-magnet machines with rotor eccentricity," IEEE Trans. Ind. Appl., vol. 48, no. 2, pp. 642–652, 2012.

[25] E. G. Strangas, S. Aviyente, and S. S. H. Zaidi, "Time-frequency analysis for efficient fault diagnosis and failure prognosis for interior permanent-magnet AC motors," *IEEE Trans. Ind. Electron.*, vol. 55, no. 12, pp. 4191–4199, 2008.

[26] M.A.Awadallah, M.M.Morcos, S.Gopalakrishnan,andT.W.Nehl,"A neuro-fuzzy approach to automatic diagnosis and location of stator inter- turn faults in CSI-fed PM brushless DC motors," IEEE Trans. Energy Convers., vol. 20, no. 2, pp. 253–259, 2005.

[27] J. R. Riba Ruiz, J. A. Rosero, A. Garcia Espinosa, and L. Romeral, "Detection of demagnetization faults in permanent-Magnet synchronous motors under nonstationary conditions," *IEEE Trans. Magn.*, vol. 45, no. 7, pp. 2961–2969, 2009.

[28] M. A. Awadallah, M. M. Morcos, S. Gopalakrishnan, and T. W. Nehl, "Detection of stator short circuits in VSI-Fed brushless DC motors using wavelet transform," IEEE Trans. Energy Convers., vol. 21, no. 1, pp. 1– 8, 2006.

[29] S. Rajagopalan, J. A. Restrepo, J. M. Aller, T. G. Habetler, and R. G. Harley, "Nonstationary motor fault detection using recent quadratic time- frequency representations," IEEE Trans. Ind. Appl., vol. 44, no. 3, pp. 735–744, 2008.

[30] M. Delgado Prieto, A. Garcia Espinosa, J. R. Riba Ruiz, J. C. Urresty, and J. A. Ortega, "Feature Extraction of demagnetization faults in permanent- magnet synchronous motors based on box-counting fractal dimension," IEEE Trans. Ind. Electron., vol. 58, no. 5, pp. 1594–1605, 2011.

[31] Z. Jiang, X. Huang and W. Cao, "RLS-Based Algorithm for Detecting Partial Demagnetization under Both Stationary and Nonstationary Conditions", MDPI Energies, Vol. 15, No. 3509, 2022.

[32] K. N. Gyftakis, T. A. Garcia-Calva, G. A. Skarmoutsos, D. Morinigo-Sotelo, M. Mueller and R. d. J. Romero-Troncoso, "Detection and Identification of Demagnetization in PM Generators During Transient Conditions," 2021 IEEE 13th International Symposium on Diagnostics for Electrical Machines, Power Electronics and Drives (SDEMPED), pp. 345-350, 2021.

VIII. BIOGRAPHIES

K. N. Gyftakis (M'11, SM'20) received the Diploma in Electrical and Computer Engineering from the University of Patras, Patras, Greece in 2010. He pursued a Ph.D. in the same institution in the area of electrical machines condition monitoring and fault diagnosis (2010-2014). Furthermore, he worked as a Post-Doctoral Research Assistant in the Dept. of Engineering Science, University of Oxford, UK (2014-2015). Then he worked as Lecturer (2015-2018) and Senior Lecturer (2018-2019) in Coventry University, UK. Between 2015-2022 he worked as a Lecturer in Electrical Machines, University of Edinburgh.

He is currently an Associate Professor with the Technical University of Crete, Greece. His research interests focus in the fault diagnosis, condition monitoring and degradation of electrical machines. He has authored more than 120 papers in international scientific journals and conferences and chapter for the book: "Diagnosis and Fault Tolerance of Electrical Machines, Power Electronics and Drives", IET, 2018. Finally he serves as an Associate Editor for the IEEE Transactions on Energy Conversion and the IEEE Transactions on Industry Applications.

T. A. Garcia-Calva received the B.S. degree in 2014 and the M.E. (cum laude) degree in 2016 from the University of Guanajuato, México, where he is currently working toward the Ph.D. in electrical engineering. He was an intern with the Universidad de Valladolid (UVA), Spain, and with the Universitat Politècnica de València (UPV), Spain in 2016. His research interests include signal processing, spectral analysis, time-frequency distributions and condition monitoring of electrical machines.

G. A. Skarmoutsos (S'20) received the Diploma in electrical and computer engineering from the University of Patras, Greece, in 2018. He is currently working towards the Ph.D. degree in electrical engineering at the Institute for Energy Systems, the University of Edinburgh, U.K. His research interests include magnetic field computation, and fault diagnostic techniques of electric machines.

D. Morinigo-Sotelo (M'04) received the B.S.and Ph.D. degrees in electrical engineering from the University of Valladolid (UVA), Spain, in 1999 and 2006, respectively. He was a Research Collaborator on Electromagnetic Processing of Materials with the Light Alloys Division of CIDAUT Foundation since 2000 until 2015. He is currently with the Research Group on Analysis and Diagnostics of Electrical Grids and Installations (ADIRES), which belongs to the ITAP Institute (UVA), and with the HSPdigital Research Group, México. His current research interests include fault detection and diagnostics of induction machines, power quality, and smart grids.

M. Mueller received the B.Sc. (Eng.) degree from Imperial College London, London, U.K., and the Ph.D. degree from the University of Cambridge, Cambridge, U.K., in 1988 and 1991, respectively. He was a Lecturer with the School of Engineering, University of Durham, from 1997 to 2004. Since 2004, he has been with the School of Engineering, University of Edinburgh, where he holds a Personal Chair in electrical generation systems and was the Head of the Institute for Energy Systems, 2014–2018.

This article has been accepted for publication in IEEE Transactions on Industry Applications. This is the author's version which has not been fully edited and content may change prior to final publication. Citation information: DOI 10.1109/TIA.2022.3221699

R. de J. Romero-Troncoso (M'07–SM'12) received the Ph.D. degree in mechatronics from the Autonomous University of Queretaro, Queretaro, Mexico, in 2004. He is a National Researcher level 3 with the Mexican Council of Science and Technology, CONACYT. He is currently a Head Professor with the Autonomous University of Queretaro, Mexico. He has been an advisor for more than 200 theses, an author of two books on digital systems (in Spanish), and a coauthor of more than 130 technical papers published in international journals and conferences. His fields of interest include hardware signal processing and mechatronics. Dr. Romero–Troncoso was a recipient of the 2004 Asociación Mexicana de Directivos de la Investigación Aplicada y el Desarrollo Tecnológico Nacional Award on Innovation for his work in applied mechatronics, and the 2005 IEEE ReConFig Award for his work in digital systems. He is part of the editorial board of Hindawi's International Journal of Manufacturing Engineering